5284–5298 *Nucleic Acids Research, 2011, Vol. 39, No. 12* *Published online 23 February 2011*
doi:10.1093/nar/gkr072

PepFect 14, a novel cell-penetrating peptide for oligonucleotide delivery in solution and as solid formulation

Kariem Ezzat[1,*], Samir EL Andaloussi[2], Eman M. Zaghloul[2], Taavi Lehto[3], Staffan Lindberg[1], Pedro M. D. Moreno[2], Joana R. Viola[2], Tarek Magdy[1], Rania Abdo[1], Peter Guterstam[1], Rannar Sillard[1], Suzan M. Hammond[4], Matthew J. A. Wood[4], Andrey A. Arzumanov[5], Michael J. Gait[5], C. I. Edvard Smith[2,*], Mattias Hällbrink[1,6] and Ülo Langel[1,3,*]

[1]Department of Neurochemistry, Stockholm University, SE-106 91 Stockholm, [2]Department of Laboratory Medicine, Karolinska Institutet, SE-141 86 Huddinge, Sweden, [3]Tartu University, Institute of Technology, 504 11 Tartu, Estonia, [4]Department of Physiology, Anatomy and Genetics, University of Oxford, South Parks Road, Oxford, OX1 3QX, [5]Medical Research Council, Laboratory of Molecular Biology, Cambridge, CB2 0QH, UK and [6]Cepep 2, SE-104 30, Stockholm, Sweden

Received August 28, 2010; Revised January 24, 2011; Accepted January 27, 2011

ABSTRACT

Numerous human genetic diseases are caused by mutations that give rise to aberrant alternative splicing. Recently, several of these debilitating disorders have been shown to be amenable for splice-correcting oligonucleotides (SCOs) that modify splicing patterns and restore the phenotype in experimental models. However, translational approaches are required to transform SCOs into usable drug products. In this study, we present a new cell-penetrating peptide, PepFect14 (PF14), which efficiently delivers SCOs to different cell models including HeLa pLuc705 and mdx mouse myotubes; a cell culture model of Duchenne's muscular dystrophy (DMD). Non-covalent PF14-SCO nanocomplexes induce splice-correction at rates higher than the commercially available lipid-based vector Lipofectamine™ 2000 (LF2000) and remain active in the presence of serum. Furthermore, we demonstrate the feasibility of incorporating this delivery system into solid formulations that could be suitable for several therapeutic applications. Solid dispersion technique is utilized and the formed solid formulations are as active as the freshly prepared nanocomplexes in solution even when stored at an elevated temperatures for several weeks. In contrast, LF2000 drastically loses activity after being subjected to same procedure. This shows that using PF14 is a very promising translational approach for the delivery of SCOs in different pharmaceutical forms.

INTRODUCTION

Despite the tremendous success of basic biomedical research in the last decades, new-drug output from pharmaceutical companies has been constant over the last 60 years and mostly based on small molecules (1). This gap between discoveries and therapeutics has recently led to intense interest in translational research; to transform biomedical discoveries into commercializable drug products (2). One group of gene modulating agents showing great potential as therapeutic drug products is splice-correcting oligonucleotides (SCOs). Recent studies using high-throughput sequencing indicate that 95–100% of human pre-mRNAs have alternative splice forms (3). Mutations that affect alternative pre-mRNA splicing have been linked to a variety of cancers and genetic diseases, and SCOs can be used to silence mutations that cause aberrant splicing, thus restoring correct splicing and

*To whom correspondence should be addressed. Tel: +468164264; Fax: +468161371; Email: kariem@neurochem.su.se
Correspondence may also be addressed to C. I. Edvard Smith. Tel: +46858583651; Fax: +46858583650; Email: edvard.smith@ki.se
Correspondence may also be addressed to Ülo Langel. Tel: +468161793; Fax: +46816137; Email: ulo@neurochem.su.se
Present address:
Peter Guterstam, GE Healthcare Bio-Sciences, SE-751 84 Uppsala, Sweden.

function of the defective gene (4,5). One example is Duchenne's muscular dystrophy (DMD), a genetic disease that affects 1 in 3500 young boys worldwide (6). DMD is a neuromuscular disorder caused mainly by nonsense or frame-shift mutations in the dystrophin gene. SCOs are used to induce targeted 'exon skipping' and to correct the reading frame of mutated dystrophin mRNA such that shorter, partially-functional dystrophin forms are produced (7). SCOs targeting exon 51 are currently in human clinical trials in various parts of Europe to treat DMD (8,9). However, translating the promising results of SCOs into bed-side drug products requires optimization of many parameters ranging from enhancement of cellular uptake and biodistribution to pharmaceutical formulation and long-term stability.

SCOs are antisense oligonucleotides (ONs) ranging from 15 to 25 bases in length. In contrast to the normal antisense approach, SCOs must not activate RNase H, which would destroy the pre-mRNA target before it could be spliced (4,5). That is why these ONs are of different chemical nature than DNA and RNA. 2′-*O*-methyl RNA (2′-*O*Me) and phosphorothioate (PS) RNA are among the chemistries successfully utilized to induce splice-correction (4). Such chemical modifications impart better annealing with RNA and enhance the serum stability of the ONs (10). For these reasons PS-2′-*O*Me SCOs are used in this study. From a pharmaceutical perspective, PS-2′-*O*Me SCOs are to be considered class III drugs in the biopharmaceutical classification system (11), with high solubility and low permeability owing to their high molecular weight and dense charge distribution (12). That is why several methods have been devised to enhance their uptake into cells. Cationic liposomes have been routinely used as delivery vectors for ONs; however, toxicity remains a significant problem, according to several *in vivo* findings (13).

One class of vectors that appears potent for this purpose without the associated toxicity of cationic liposomes is cell-penetrating peptides (CPPs). CPPs are polybasic and/or amphipathic peptides, usually less than 30 amino acids in length, that possess the ability to translocate across cellular plasma membranes. They have gained much attention in recent years due to their ability to efficiently and safely deliver an array of therapeutic cargos, from small molecules to nanopaticles both *in vitro* and *in vivo* (14,15). For splice-correction, CPPs covalently conjugated to different SCOs have been reported to successfully induce splice-correction in different models (7,16). However, despite being less toxic, the transfection efficiencies reported have generally been less than those achieved utilizing lipid-based vectors such as (LF2000) (17). Interestingly, some CPPs have been successfully exploited for ON delivery using a non-covalently complexation strategy (18). Having net positive charge, such CPPs have been shown to form nano-sized complexes with negatively charged ONs, which are efficiently internalized by cells presumably via an endocytosis-dependant mechanism (15,18,18,19). The non-covalent complexation strategy has the advantage of avoiding laborious chemical conjugation of the CPP with its cargo. Moreover, it was found that lower concentrations of ONs are generally required to achieve a biological response utilizing the non-covalent complexation (17,19). However, one limitation of this strategy is that much of the delivered cargo becomes entrapped in endosomes following endocytosis. Therefore, several chemical modifications have been introduced into CPPs to enhance endosomal escape (19). N-terminal stearic acid modification was shown to enhance both the complexation capacity and endosomal escape properties of certain CPPs (19,20). It has been shown previously by our group that the stearic acid-modified CPPs, stearyl-TP10 (21) and stearyl-(RxR)4 (17), are able to transfect cells with PS-2′-*O*Me SCOs . However, a drawback with the above-mentioned peptides is that they are generally less efficient than commercial lipid-based vectors such as LF2000, and relatively inefficient at transfecting cells in the presence of serum proteins.

Although CPPs have been extensively studied as drug delivery vectors, formulation of CPP-based therapeutics into different pharmaceutical forms has never been given the same attention. Pharmaceutical formulation has always a major influence on the efficiency and stability of active pharmaceutical ingredients. In addition, each therapeutic application requires its own pharmaceutical form. Therefore, developing different formulations for CPP-based therapeutics could have great implications on their activity and stability, besides, broadening the range of therapeutic applications that CPPs could be utilized in. Particularly, solid formulation is the most widely used pharmaceutical form. It is used in tablets, capsules, sustained-release formulations, powders for inhalation and powders for injection. In addition, solid formulations are the most stable forms upon storage and transport. Thus, from a translational perspective, it would be of great importance to be able to formulate CPP-based therapeutics as solid form.

Here, we describe a new stearylated CPP that we designate PepFect 14 (PF14). It is a modified version of our previously reported peptide, stearyl-transportan10 (stearyl-TP10) (21), where we utilized ornithines and leucines instead of lysines and isoleucines. PF14 demonstrates remarkable splice-correction activity in two different cell models including mdx mouse myotubes, a cell culture model of DMD, even in the presence of serum. Furthermore, the feasibility of formulating these nanocomplexes into solid formulation was investigated and the efficiency and stability of such formulations were assessed. Remarkably, the solid formulations obtained upon drying the nanocomplexes over soluble excipients were as active as the freshly prepared counterpart even when stored at elevated temperatures for several weeks.

MATERIALS AND METHODS

Oligonucleotide and peptide synthesis

PS-2′-*O*-methyl RNA ON (Table 1) was synthesized on an ÄKTA^{TM} oligopilot^{TM} plus 10 synthesizer with Oligosynt^{TM} 15 (GE Healthcare, Sweden) pre-packed synthesis columns as previously described (22). For 5′-labeling, a molar excess of 10 equivalents Cy5-amidite (GE Healthcare, UK) at 0.1 M was used and Cy5-amidite

Table 1. Sequences of PF14 and PS-2′-*O*-methyl oligoribonucleotides

Name	Sequence
PF14	Stearyl- AGYLLGKLLOOLAAAALOOLL-NH2
PF14 A	AGYLLGKLLOOLAAAALOOLL-NH2
SCO for HeLa pLuc705 cells	5′-CCU CUU ACC UCA GUU ACA
SCO for mdx mouse myotubes	5′-GGCCAAACCUCGGCUUACCU

coupling proceeded for 10 min. The crude ON was purified by anion-exchange chromatography and desalting followed by anion-exchange high-performance liquid chromatography (HPLC) and mass analysis as previously described (22). The molarity of ONs was determined by measurements of optical density at 260 nm. The PS-2′-*O*-Me RNA ON for mdx mouse myotubes (Table 1) with sodium counterions was obtained from RiboTask (23). PF14 (Table 1) was synthesized (SYRO multiple peptide synthesizer, MultiSynTech, Germany) on Fmoc-Rink-amide-4-methylbenzhydrylamine resin (0.67 mmol/g, IRIS Biotech, Germany) using standard Fmoc solid-phase peptide synthesis (24). Stearic acid (Sigma-Aldrich) was coupled to the N-terminus by using TBTU/HOBt [2-(1H-benzotriazole-1-yl)-1,1,3,3-tetramethyluronium tetrafluoroborate/1-hydroxybenzotriazole] (IRIS Biotech, Germany) activation in dimethylformamide/dichloromethane. The peptide was cleaved using 95% TFA/2.5% water/2.5% triisopropylsilane for 3 h and precipitated in diethylether. The obtained crude peptide was dried in vacuum overnight. The peptide was purified by HPLC on a Discovery® C-18 Supelco® column (Sigma-Aldrich, Sweden) using a gradient of acetonitrile/ water containing 0.1% TFA. The identity of the purified product was verified by analytical HPLC and by Perkin Elmer prOTOF™ 2000 matrix-assisted laser desorption ionization time-of-flight mass spectrometer (Perkin Elmer, Sweden). The mass-spectrum was acquired in positive ion reflector mode using α-cyano-4-hydroxycinnamic acid as a matrix (Sigma-Aldrich) (10 mg/ml, 7:3 acetonitrile: water, 0.1% TFA). The molarity of the peptide was determined based on dilutions of accurately weighed substances.

Cell culture

HeLa pLuc705 cells, kindly provided by Prof. R. Kole, and U2OS cells were grown at 37°C, 5% CO_2 in Dulbecco's Modified Eagle's Medium (DMEM) with glutamax supplemented with 0.1 mM non-essential amino acids, 10% fetal bovine serum (FBS), 200 U/ml penicillin and 200 μg/ml streptomycin (Invitrogen, Sweden). Mdx mouse myotubes were obtained from confluent H2K mdx cells seeded in gelatin-coated 24-well plates following 2 days of serum deprivation (DMEM with 5% horse serum) (25). More information regarding cell culture and myotubes development can be found in Supplementary Figure S1.

Splice-correction assay

HeLa pLuc705 cells (5×10^4) were seeded 24 h prior to experiments into 24-well plates. PS-2′-*O*Me SCOs were mixed with PF14 at different molar ratios (MRs) in MQ-water in 10% of the final treatment volume (i.e. 50 μl). Complexes were formed for 1 h at room temperature and meanwhile the cell medium was replaced in the wells with fresh serum-free or serum-containing DMEM media (450 μl). Thereafter, complexes were added to each well. When using LF2000, Oligofectamine, Lipofectamine™ RNAiMAX (Invitrogen, Sweden) and jetPEI (Polyplus transfection, *In Vitro*, Sweden), the complexes were prepared according to the manufacturer's protocol. Cells were treated with PF14-SCO nanocomplexes at different MRs (3:1, 5:1, 7:1, 10:1, 20:1) for 4 h in serum-free medium (or in serum-containing media) followed by addition of serum to a final concentration of 10% (only to cells grown in serum-free medium) and incubated for additional 20 h. Thereafter, the cells were lysed using 100 μl 0.1% Triton X-100 in HEPES-buffered Krebs Ringer (HKR) buffer for 30 min at room temperature. Luciferase activity was measured using Promega's luciferase assay system on GLOMAX™ 96 microplate luminometer (Promega, Sweden) and normalized to protein content determined using the Lowry method (BioRad, USA). In experiments with chloroquine, after complex formation and prior to treatment of cells, chloroquine (final concentration 100 μM) was added to the transfection mixture in order to promote endosomal escape. Four hours after addition of the nanocomplexes and chloroquine to cells, cell medium was replaced with fresh medium in order to avoid the toxic effects of chloroquine. In experiments assessing the impact of temperature on splice correction, cells were kept for 30 min at 37 or 4°C prior to addition of PF14-SCO complexes. Cells were treated for 1 h, washed twice with PBS and cultivated back at 37°C for additionally 20 h. For experiments with mdx mouse myotubes, PF14 nanocomplexes at different MRs were prepared as mentioned above and incubated with myotubes for 4 h in 0.5 ml OptiMEM or in DMEM/10% FBS. ONs complexed with Lipofectamine 2000 in OptiMEM according to the manufacturer's protocol, were also incubated with myotubes in OptiMEM as a control. The media in all cases was replaced by 1 ml of DMEM/5% horse serum media for further incubation.

Reverse-transcription PCR

For the HeLa pLuc705 cell-line, cells were trypsinized and total RNA was isolated from the cell pellets using the RNeasy plus kit (QIAGEN, Sweden). The quality of RNA was verified by agarose gel electrophoresis. Three nanogram of RNA were used in each reverse-transcription PCR (RT–PCR) reaction in which the total volume was 20 μl using the ONE STEP RT–PCR kit (QIAGEN). The primers had the following sequences: Fwd-5′-TTGATAT GTGGATTTCGAGTCGTC-3′; Rev-5′-TGTCAATCAG AGTGCTTTTGGCG-3′. The program for the RT–PCR was as follows: 55°C, 35 min, then 95°C, 15 min, for reverse transcription step directly followed by the PCR

(94°C, 30 s, then 55°C, 30 s, then 72°C, 30 s) for 30 cycles and finally 72°C, 10 min, for final extension. The PCR products were analyzed in a 2% agarose gel in 1 × TBE buffer and visualized by SYBR Gold (Invitrogen, Molecular Probes) staining. Gels were documented using the Fluor-S system with a cooled CCD camera (BioRad) and analyzed with the Quantity One software (BioRad). For the mdx mouse myotubes, 24 h after transfection myotubes were washed twice with PBS and total RNA was extracted with 0.5 ml of TRI Reagent (Sigma). RNA preparations were treated with RNase free DNase (2 U) and Proteinase K (20 μg) prior to RT–PCR analysis. RT–PCR was carried out in 12.5 μl with 0.5 μg RNA template using SuperScript III One-Step RT–PCR System with Platinum Taq DNA polymerase (Invitrogen) primed by forward primer 5′-CAG AAT TCT GCC AAT TGC TGAG-3′ and reverse primer 5′-TTC TTC AGC TTG TGT CAT CC-3′. The initial cDNA synthesis was performed at 55°C for 30 min followed by 30 cycles of 95°C for 30 s, 55°C for 1 min and 68°C for 80 s. RT PCR product (1 μl) was then used as the template for secondary PCR performed in 25 μl with 0.5 U Super TAQ polymerase (HT Biotechnologies) and primed by forward primer 5′-CCC AGT CTA CCA CCC TAT CAG AGC-3′ and reverse primer 5′-CCT GCC TTT AAG GCT TCC TT-3′. The cycling conditions were 95°C for 1 min, 57°C for 1 min and 72°C for 80 s for 25 cycles. Products were examined by 2% agarose gel and after scanning using Gene Tools Analysis Software (SynGene), the relative amount of exon 23 skipping was expressed as a percentage at a given concentration of conjugates averaged over duplicates of three experiments.

Fluorometry and live-cell confocal imaging

HeLa pLuc705 cells (5×10^4) were seeded 24 h before the experiment in 24-well plates. PF14-Cy5-labeled SCO nanocomplexes (MR5, 200 nM SCO) were added to the cells in 500 μl serum-free medium for 4 h followed by the addition of serum to a final concentration of 10% and incubated for additional 20 h. Cells were washed twice in HKR buffer and trypsinized for 10 min with 0.25% trypsin (Invitrogen, Sweden). Cells were then centrifuged at 1000*g* for 5 min at 4°C, and cell pellets were lysed in 250 μl 0.1% Triton X-100 in HKR buffer for 1 h, after which 200 μl lysate was transferred to a black 96-well plate. Fluorescence was measured at 650/670 nm on FlexStation II fluorescence reader (Molecular devices, USA) and the amount of internalized compound was normalized to the amount of protein was determined using the Lowry method (BioRad, USA). In experiments where splice-correction was measured simultaneously, luciferase activity was measured as mentioned above for the same cell lysate. For live cell confocal imaging microscopy studies, a number of 3.6×10^4 U2OS cells were seeded in an 8-well IBItreat μ-Slide (IBIDI; LRI instruments AB; Stockholm, Sweden), the day before the experiment. PF14-Cy5-labeled SCO complexes (MR5, 100nM SCO) and 5 μM of 10 KDa A488-Dextran (Molecular Probes, Invitrogen) were added to the cell medium and co-incubated for 3 h. Cells were then washed extensively with 1 × HBSS and finally 300 μl of OptiMEM without phenol red (Invitrogen) was added. Live cell imaging was then performed using a Zeiss LSM 510 confocal microscope equipped with a Plan-Apochromat 63 × /1.4 oil DIC objective with a 0.8 aperture. Images were analyzed and prepared with Zeiss LSM image browser or ImageJ (when imageJ was used the function despeckle was utilized to reduce noise in the image)

Cell proliferation Wst-1

Cell proliferation was assessed by the Roche Wst-1 proliferation assay according to the manufacturer's instructions. Briefly, 1×10^4 cells were seeded 1 day prior to the experiment on a 96-well plate. Cells were treated with PF14-SCO nanocomplexes at different MRs for 4 h in serum-free medium followed by the addition of serum to a final concentration of 10% and incubated for additional 20 h. LF2000 was used according to the manufacturer's protocol in serum-free conditions utilizing the same SCO dose. Wst-1 was added according to the manufacturer's protocol (Roche Diagnostics Scandinavia AB, Sweden). Wst-1 measures the activity of the mitochondrial dehydrogenases to convert tetrazolium salts to formazan and cell proliferation is directly correlated to the amount of formazan dye that is formed. Absorbance was measured at 450 nm on Digiscan absorbance reader (Labvision via AH Diagnostics AB, Sweden). The percentage of viable cells was determined by normalizing the values obtained for treated cells with untreated cells.

Solid dispersion

Excipient solutions of lactose monohydrate (Merck Chemicals, Germany), mannitol (Duchefa Biochemie, Holland) and PEG 6000 (Sigma-Aldrich, Sweden) were prepared at final concentration of 100 mg/ml in MQ water. PF14-SCO nanocomplexes (MR5, 200 nM) were prepared in 5% of the final treatment volume (i.e. 25 μl). After complexation, different proportions of the excipient solutions were added to the final concentrations of 1.67, 3.33 and 5% solubilized excipient in the reaction mixture. The mixture was thereafter dried in Savant DNA speed-vac (model DNA 120–230) for 2 h, during which the temperature ranged between 55 and 60°C. Before transfection, the dried powder was reconstituted in 50 μl of MQ water and added to cells grown in 450 μl of serum-containing medium and incubated for 24 h. LF2000 complexes were prepared according to manufacturer's protocol. Subsequently, the same proportions of the excipient solutions utilized for PF14 formulation were added, and then the mixture was dried and reconstituted similarly. Luciferase activity was measured as stated earlier.

Dynamic light scattering and zeta potential studies

Hydrodynamic mean diameter of the nanocomplexes was determined by dynamic light scatter (DLS) studies using a Zetasizer Nano ZS apparatus (Malvern Instruments, UK). PF14-SCO nanocomplexes, freshly prepared in solution or in solid dispersion (SD) formulations, were prepared

according to the protocols for transfection and diluted in Opti-MEM® with 10% serum into a final volume of 500 µl. Samples were assessed in disposable low-volume cuvettes. All data was converted to 'relative intensity' plots from where the mean hydrodynamic diameter was derived.

Zeta potential was measured in OptiMEM supplemented with 10% FCS or in 0.01 mM KCl. Measurements were performed utilizing the abovementioned instrument, set to automode and a number of five runs.

Stability study

Lactose solid dispersion formulations at a concentration of 3.33% were prepared according to the protocol for transfection and stored either at room temperature or in ovens of adjusted temperatures (40 and 60°C). Samples were monitored for 8 weeks and tested at 0, 2, 4 and 8 weeks time points.

Statistics

Values in all experiments are represented as mean ± SEM of at least three independent experiments done in duplicate. Differences were considered significant at $*P < 0.05$ using two-tailed Student's *t*-test.

RESULTS

PF14 efficiently induces SCO-mediated splice-correction in serum-free and serum-containing media in HeLa pLuc705 cell model

To screen for the most optimal peptide-SCO ratio for splice-correction activity, PF14-SCO complexes were formed at different MRs. MR 3, 5, 7 and 10 were tested in serum-free medium and MR 3, 5, 10 and 20 were tested in serum-containing medium with dose titrations using 200, 100 or 50 nM SCO. LF2000 was used as positive control in all experiments according to manufacturer's protocol utilizing the highest dose (200 nM SCO). The assay we used is based on the HeLa pLuc705 cell-line stably transfected with a luciferase-encoding gene interrupted by a mutated β-globin intron 2. This mutation causes aberrant splicing of luciferase pre-mRNA resulting in the synthesis of non-functional luciferase (26). Masking the aberrant splice site with PS-2′-*O*Me SCO redirects splicing towards the correct mRNA and consequently restores luciferase activity. We found that splice-correction was induced in a dose-dependent manner at all the tested MRs and using MR5 resulted in the highest splice-correction activity in both types of media. Remarkably, in serum-free medium, PF14 at MR5 exceeded LF2000 by several times (Figure 1A). Interestingly, in serum-containing medium, PF14 at MR5 was capable of retaining >75% of its activity observed in serum-free conditions, and also significantly surpassing LF2000 (Figure 1B).

EC_{50} and kinetics of PF14-SCO mediated splice-correction

Next, RT–PCR was conducted to assess the EC_{50} of PF14 nanocomplexes. EC_{50} is the concentration of SCO at which 50% splice-correction occurs. It is a very important parameter in the characterization of a delivery vector, because it allows direct comparison of the efficiencies of different vectors tested using the same model. RT–PCR was utilized to detect the quantity of corrected full-length luciferase mRNA after dose titration with different SCO concentrations complexed with PF14 at MR5. We found that PF14-SCO nanocomplexes have very low EC_{50} values (~100 nM) in both serum-free and serum-containing medium (Figure 2A).

In order to assess the kinetics of splice-correction, cells were transfected with PF14 at MR5 using 200 nM SCO and then the percent of splice-correction was monitored over a time interval ranging from 2 h to 48 h. More than 60% splice-correction was observed already after 8 h (Figure 2B). This shows that, although PF14 forms stable and highly active nanocomplexes with SCOs, the SCO cargo is released quickly inside the cells resulting in an early onset of the biological activity. The splice-correction activity reached its peak after 24 h before it started to decline within 48 h (Figure 2B).

PF14 efficiently induces SCO-mediated splice-correction in serum-free and serum-containing media in differentiated mdx mouse myotubes

The leading cell-model system for development of drugs and drug delivery systems for treatment of DMD is the H2K mdx mouse myotubes, which carries a point mutation in exon 23 of the dystrophin gene (25). PF14-SCO nanocomplexes at MR5 (Figure 3A and B) or MR7 (Figure 3C) were incubated with mouse mdx muscle cells at various concentrations in the presence or absence of 10% FBS. Significant amounts of exon skipping were observed, which increased in a concentration-dependent manner. For MR5, the levels were as good as treatment with the same concentration of SCO using LF2000, both in OptiMEM (serum-free conditions), and at MR7, PF14 was higher than LF2000 (Figure 3B and C). The effect of added 10% FBS was small on exon skipping at both MRs and especially at MR7, showing that PF14 activity is not substantially affected by serum.

PF14-SCO nanocomplexes are internalized via endocytosis

Subsequently, Cy5-labeled SCOs were used to determine the relation between the quantity of SCOs taken up by the cells and the biological activity. PF14 mediated uptake of Cy5-labeled SCO in a dose-dependent manner, which was congruent to the splice-correction data obtained simultaneously (Figure 4A). However, in the presence of chloroquine, the splice-correction activity increased, while the uptake remained nearly unchanged. This discrepancy between uptake and biological activity in the presence of chloroquine, a well-known endosomolytic agent, suggests the involvement of endocytic vesicles in the uptake of the nanocomplexes. Endocytic uptake was further supported by the significant decrease in activity after incubation at 4°C which is known to inhibit energy-dependant uptake mechanisms like endocytosis (Figure 4B). To further corroborate these results, live cell confocal imaging

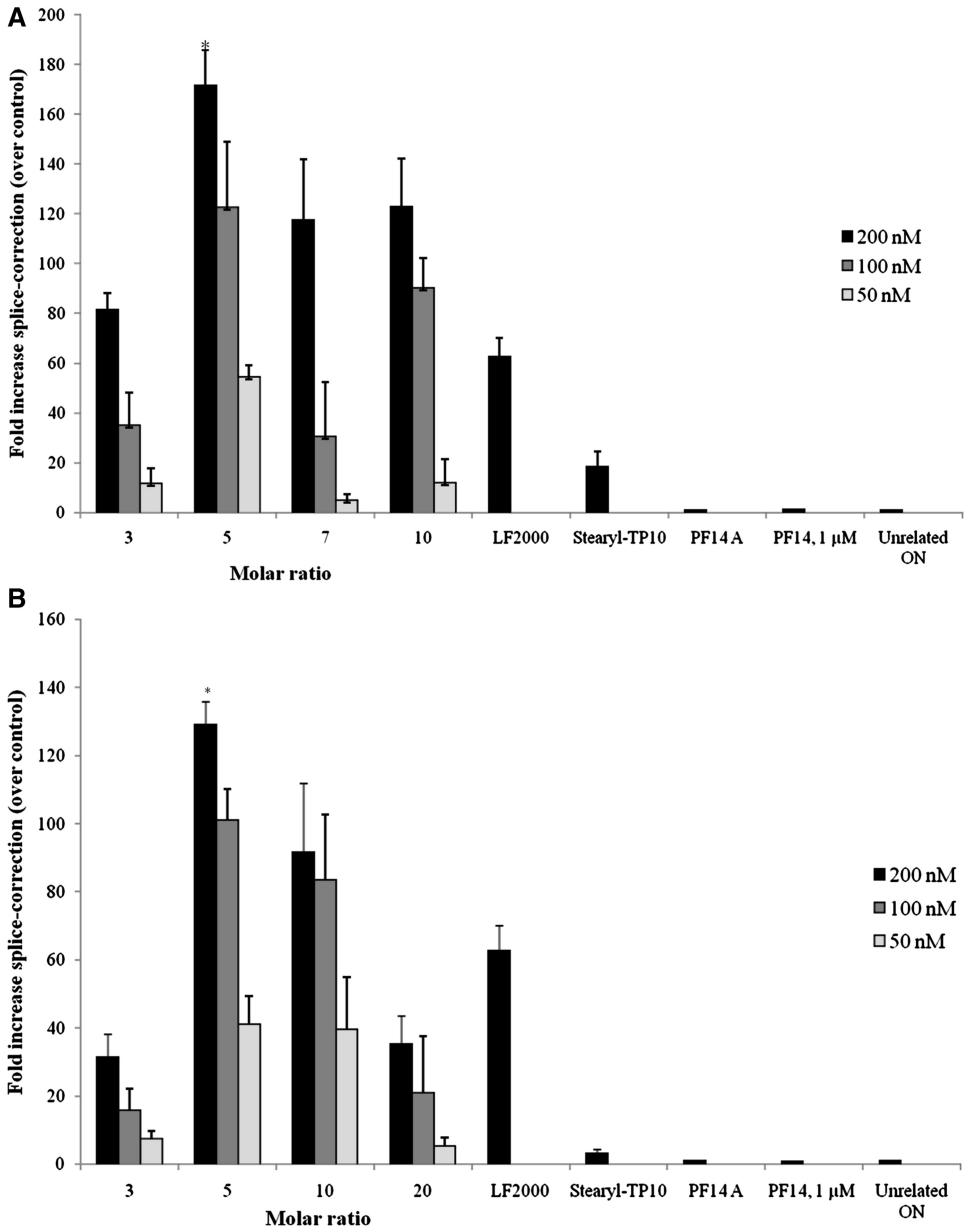

Figure 1. Splice-correction activity of PF14- SCO nanocomplexes in HeLa pLuc705 cell-line. HeLa pLuc705 cells (5×10^4) were seeded 24 h prior to experiments into 24-well plates. Cells were treated with PF14-SCO nanocomplexes at three different concentrations at MRs (3:1, 5:1, 7:1 and 10:1) for 4 h in serum-free medium followed by addition of serum to final concentration of 10% and incubated additionally for 20 h (**A**), and at MRs (3:1, 5:1, 10:1 and 20:1) for 24 h in serum-containing medium (**B**). The controls used were: stearyl-TP10 (MR5, 200 nM), PF14 A (unstearylated PF14, Table 1) at MR5 and 200 nM dose, PF14 only (1 μM) and P14-unrelated ON (MR5, 200 nM). LF2000 was used according to the manufacturer's protocol using the highest SCO concentration (200 nM). Cells were lysed in 0.1% Triton X-100 and luciferase activity was measured. Splice-correction assay results are presented as fold-increase over untreated cells (control). The values represent the mean of at least three experiments performed in duplicate (mean ± SEM, $n = 3$). Intergroup differences were considered significant at $^*P < 0.05$ using Student's *t*-test.

experiments were performed where PF14-Cy5-labeled SCO nanocomplexes together with labeled dextran were co-incubated with U2OS cells and extensive co-localization was observed (Figure 4C). Similar pattern was also seen in the A549 cell-line (Supplementary Figure S3). In addition, flow-cytometry analysis was carried out to assess the percentage of cells being transfected. In keeping with the high splice-correction activity, we found that PF14 transfected nearly the entire cell population (Supplementary Figure S4).

PF14 induces SCO-mediated splice-correction in a confluence-independent and non-toxic manner

It is a well-known fact that many commercial transfection reagents, such as LF2000, are strictly dependent on certain cell densities for optimal performance. To assess the effect of cell confluency, transfections were carried out at different cell densities (2.5×10^4, 5×10^4, 10×10^4 and 20×10^4 cells/well), comparing PF14 with LF2000. As shown in Figure 5A, PF14-SCO complexes appeared less sensitive

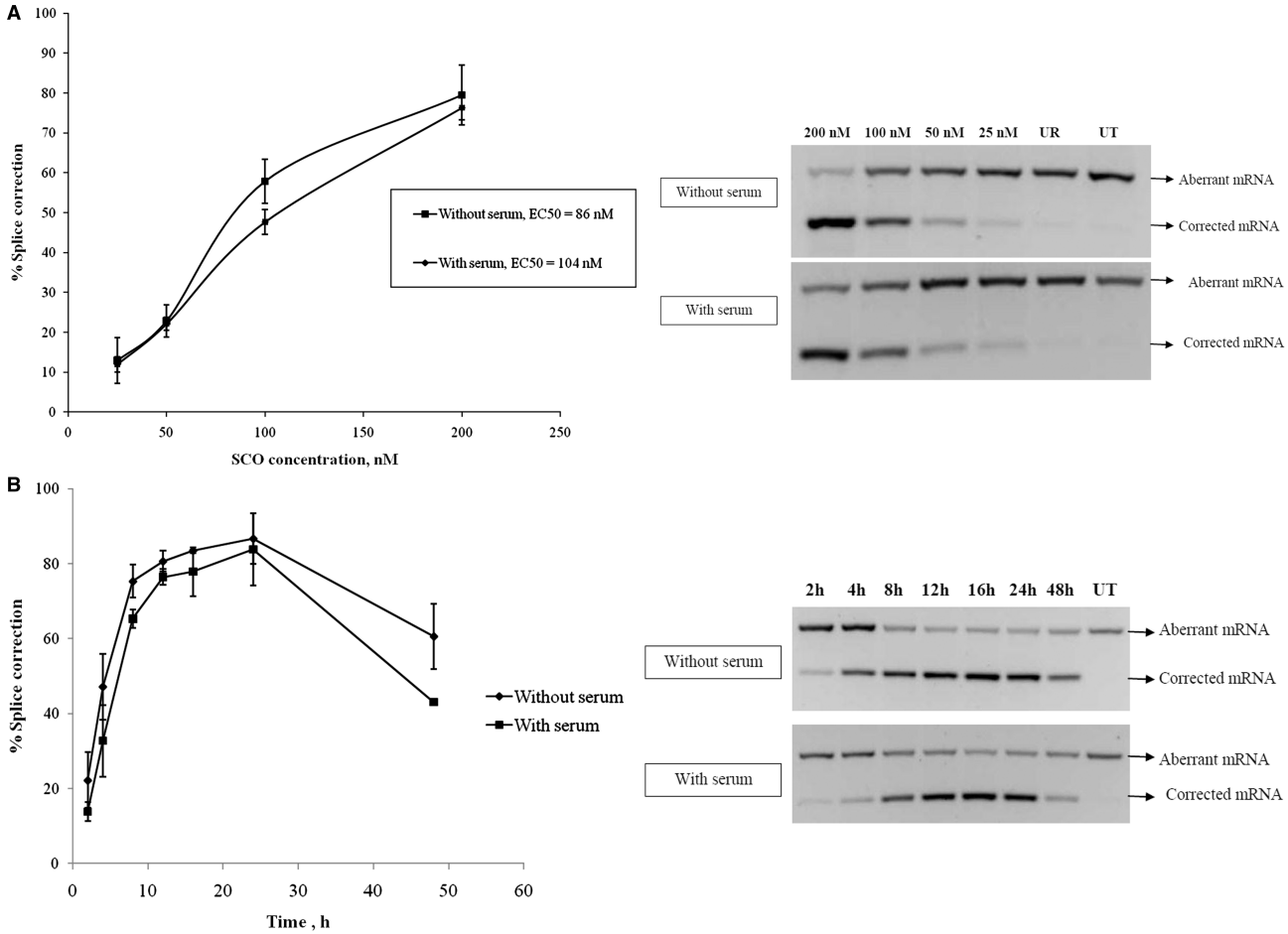

Figure 2. EC50 and kinetics of PF14 SCO nanocomplexes. (**A**) The concentration of SCO at which 50% splice-correction occurred is referred to as EC50. HeLa pLuc705 cells were transfected with different concentrations of SCO (25–200 nM) formulated with PF14 at MR5. The control, unrelated ON was used at the highest concentration tested (200 nM). Splice-correction was evaluated by measuring the corrected mRNA levels after running RT–PCR. (i) Splice-correction induced by different concentrations of the SCO. Cells were transfected with PF14 nanocomplexes in either serum-free medium (without serum) or in serum-containing medium (with serum) according to the transfection protocol stated earlier. Splice-correction was calculated as the percentage (percent splice-correction) of the corrected luciferase band to the sum of corrected and aberrant bands. (ii) Levels of corrected mRNA were quantified in 2% agarose gel using the Quantity One software. Gels are for nanocomplexes with PF14 without serum (top) and PF14 with serum (bottom). Lanes are as follows: 200 nM SCO, 100 nM SCO, 50 nM SCO, 25 nM SCO, 200 nM unrelated SCO (UR) and untreated cells (UT). The upper band in each gel represents the aberrant luciferase mRNA and the lower band is for the corrected form. (**B**) (i) Kinetics of splice-correction in HeLa pLuc705 cells. The SCO was complexed with PF14 at MR5. Final concentration of the SCO in each well was 200 nM. Transfections were performed in either serum-free (without serum) or serum-containing (with serum) media. (ii) Gels are for complexes with PF14 without serum (top) and PF14 with serum (bottom). Lanes are as follows: 2, 4, 8, 12, 16, 24, 48 h and untreated cells (UT).

to variation in cell density compared to LF2000, which progressively lost its activity as the cell number increased. In order to exclude that the high transfection efficiency observed with PF14 was associated with increased cytotoxicity, the activity of mitochondrial dehydrogenases was measured as an indicator of healthy, metabolically active cells using the Wst-1 assay. Even under serum-free conditions (Figure 5B), PF14-SCO complexes had no effect on cell viability, whereas LF2000 induced significant impairment of metabolic activity; a well-known problem of lipid-based ON complexes (lipoplexes) (13).

PF14-SCO nanocomplexes can be formulated into solid form by solid dispersion technique

To investigate the possibility of formulating PF14-SCO nanocomplexes into solid formulation, we adopted the solid dispersion technique. This technique was used to obtain uniform distribution of the nanocomplexes over hydrophilic solid matrices. Mannitol, lactose and PEG 6000 were used as excipients at various concentrations: 1.67, 3.33 and 5 % solubilized excipient in the reaction mixture (referred to as low, medium and high concentrations of excipient, respectively, Figure 6). For drying, we used heating to 55–60°C under vacuum. We found that, after resuspension and addition to the cells, the solid formulations were remarkably efficient at inducing splice-correction at rates comparable to the freshly prepared nanocomplexes in solution (Figure 6). Actually, lactose solid dispersion at a concentration of 3.33% (lactose-SD 3.33%) mediated splice-correction activity almost identical to the freshly prepared nanocomplexes. Mannitol solid dispersions displayed slightly lower values, while PEG

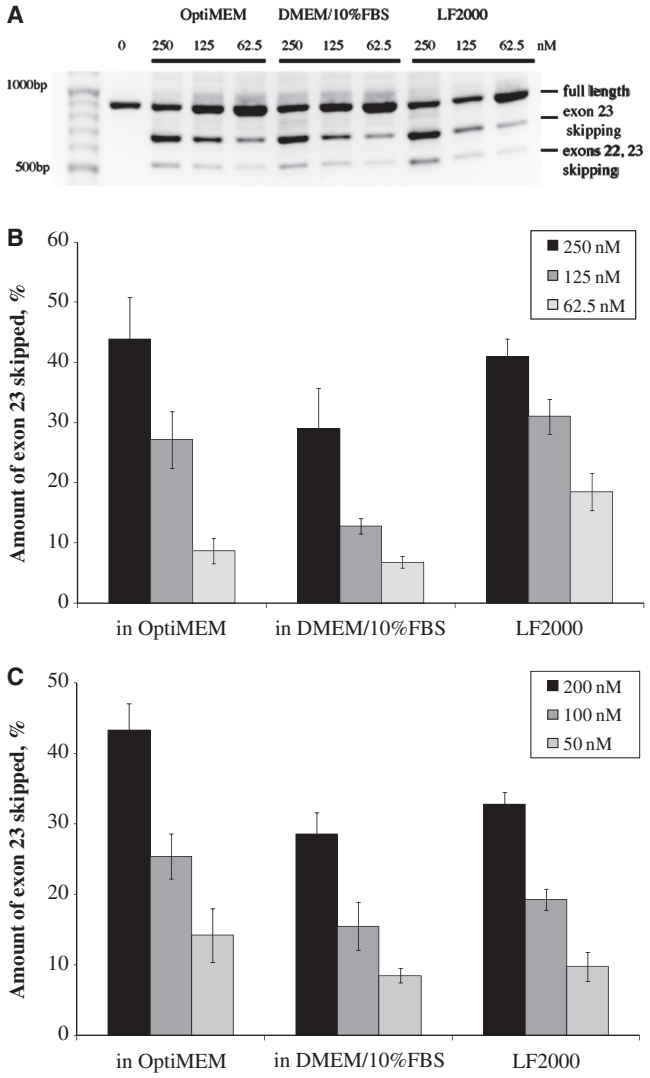

Figure 3. Splice-correction activity of PF14-SCO nanocomplexes in mdx mouse myotubes. (**A**) RT–PCR analysis to measure exon skipping activity of PF14-SCO nanocomplexes in mdx mouse myotubes at three different concentrations, at MR5 in serum-free OptiMEM and DMEM/10% FBS in comparison with control LF2000 transfection in OptiMEM. Exon skipping activity was measured as the amount of RT–PCR product after treatment of cells with PF14-SCO nanocomplexes at MR5 (**B**) or MR7 (**C**) at three different concentrations. The values represent the mean of at least three independent experiments performed in duplicate (mean ± SEM, $n = 3$).

6000 solid dispersions demonstrated the highest deviation from the values obtained using the freshly prepared nanocomplexes (Figure 6). In contrast, applying the same procedure on LF2000 nearly eliminated any residual activity. On the contrary, the high residual activity of PF14 formulations suggests that the PF14 nanocomplexes remain intact after drying and dispersion under these conditions.

DLS analysis and zeta potential measurements of PF14-SCO nanocomplexes

To confirm the presence of intact nanocomplexes in the formulations, DLS studies and zeta potential measurements were performed. These assessments were conducted in the presence of serum to allow possible correlations between such parameters and transfection activity at physiological conditions. Serum contains a number of proteins and protein aggregates that will scatter light resulting in a population of particles independent of the PF14-SCO nanocomplexes and can also affect the zeta potential by surface adsorption of some serum proteins. However, we believe that although the presence of serum will affect such measurements, these conditions are more relevant to the physiological ones. For DLS, we have compared the populations detected in serum-containing medium alone and after addition of PF14-SCO nanocomplexes. It was possible to distinguish the constant protein aggregates (inherent to the serum, and >100 nm) and a completely independent population associated to the PF14 nanocomplexes (data not shown). Due to the presence of serum proteins, the polydispersity index (PdI) of the solution containing the nanocomplexes does not describe the homogeneity of the PF14 nanocomplexes alone. For this reason, we refer to the shape of the curves that characterize the different populations while evaluating the homogeneity of the particles. For zeta potential, measurements were carried out either in 0.01 mM KCl or in the presence of 10% serum. After resuspension of the solid formulations, DLS measurements showed that nanocomplexes are present in all the tested formulations. However, the uniformity of particles size distribution and the extent of similarity in relation to the freshly prepared nanocomplexes differed with different excipients. Lactose-SD 3.33% formulations were most homogeneous and most similar to the distribution pattern of the freshly prepared nanocomplexes in solution (Figure 7 and Table 2). These results go in accordance with the transfection results where lactose-SD 3.33% displayed the highest splice-correction activity. Moreover, this analysis demonstrates that different excipients affect the physicochemical characterizes of the nanocomplexes differently in terms of particle size and uniformity, and this effect is reflected on the biological activity. We studied the surface charge (zeta potential) of the PF14 nanocomplexes, both freshly prepared and after drying at 50–60°C in the solid dispersion procedure. Interestingly, independent of formulation type and media (presence or absence of serum), the nanocomplexes displayed negative surface charges (Table 2).

Solid dispersion formulations are stable for several weeks at elevated temperatures

Finally, we tested the stability of the best-performing formulation, lactose-SD3.33%, when stored for 2 months at an elevated temperatures. The formulations were stored at three different temperatures (RT, 40 and 60°C) and sampled over an 8 weeks period. We found that the tested formulations were remarkably stable. There was no statistically significant loss in transfection efficiencies at any time-point except for the 60°C 8-weeks point where the transfection efficiency decreased to 70% of the initial value (Figure 8). Compared to lyophilized lipoplexes (27,28), PF14 formulations demonstrated an excellent

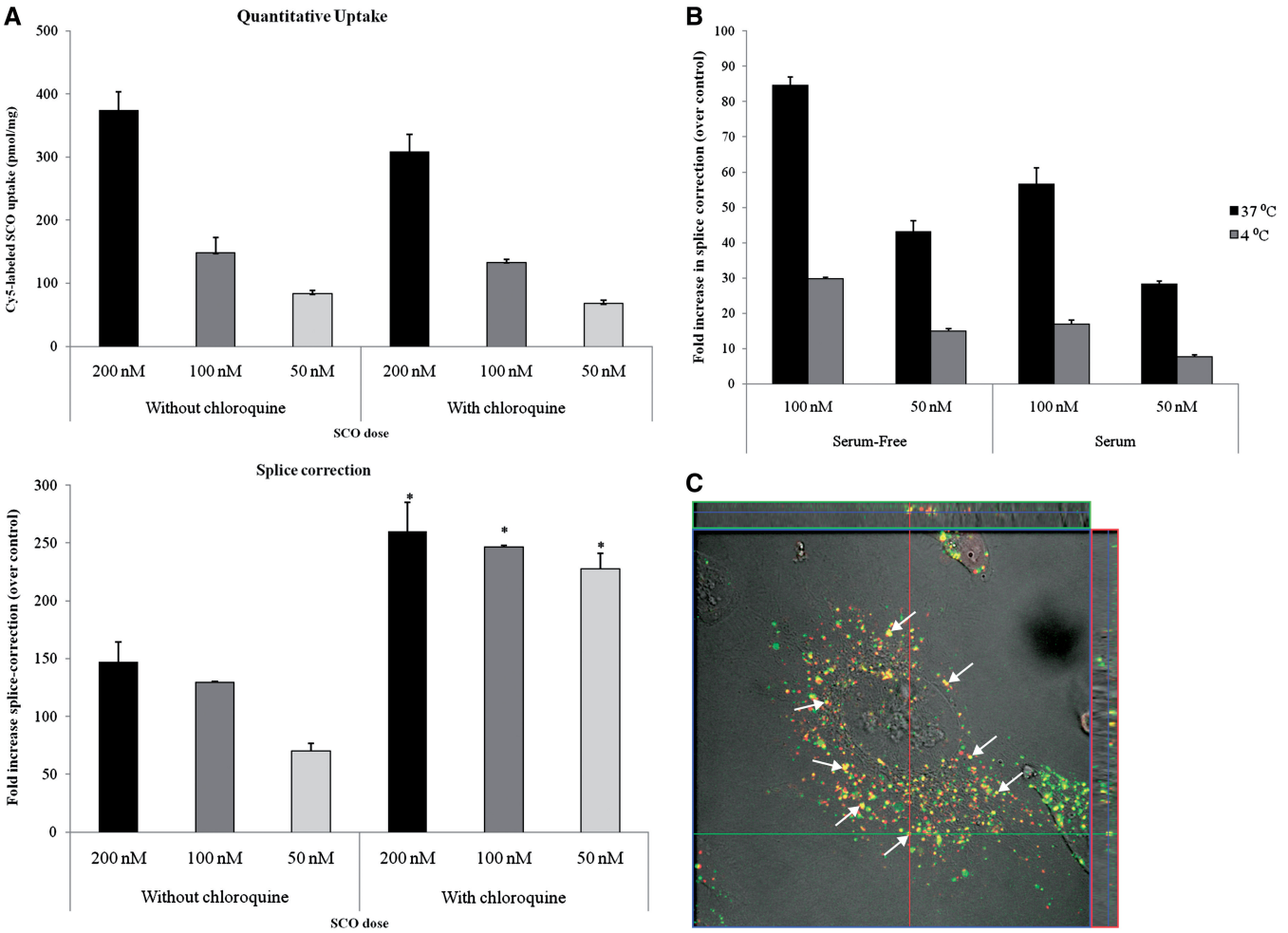

Figure 4. Uptake of Cy5-labeled SCO, effect of lowering temperature and live cell confocal imaging. (**A**) HeLa pLuc705 cells (5×10^4) were seeded 24 h prior to experiments into 24-well plates. Cells were treated with PF14-Cy5-lebeled SCO nanocomplexes at MR5 at three different concentrations for 4 h in serum-free medium followed by the addition of serum to a final concentration of 10% and incubated for additional 20 h. For the chloroquine-treated wells, 100 μM chloroquine was added to the complexes prior to cell treatments. Cells were washed with HKR buffer, trypsinized and centrifuged at 1000*g*. Pellets were lysed in 0.1% Triton X-100 in HKR buffer and fluorescence was measured at 650/670 nm. (i) Fluorescence was recalculated to pmol internalized Cy5 SCO per mg protein. (ii) Luciferase activity was measured for the same cell lysate. The values represent the mean of at least two independent experiments performed in triplicate (mean ± SEM, $n = 3$). Intergroup differences were considered significant at $^*P < 0.05$ using Student's *t*-test. (**B**) HeLa pLuc 705 cells (5×10^4) were seeded 24 h prior to experiments into 24-well plates. Thirty minutes prior treatment of cells with 50 or100 nM PF14-SCO (MR5) in serum or serum-free media, cells were incubated at 4 or 37°C. Cells were treated for 1 h at indicated temperatures and washed twice with PBS before being placed back at 37°C for additionally 20 h. Cells were processed and analyzed as in the chloroquine experiements. (**C**) PF14-Cy5-SCO complexes and 10 kDa A488-Dextran were co-incubated with U2OS cells. A major co-localization is seen overall, presented by the appearance of yellow colored vesicles (co-localization of green marked Dextran and red marked PF14-SCO nanocomplexes). The white arrows point out some pre-eminent co-localization vesicles. Several *Z*-slices per image were taken which allowed us to confirm the co-localization both in *X*, *Y* and *Z* plane in more detail. Such an example is given by the intersection of the green/red (*X*, *Y* plane; main picture) and green/blue (*Z* sectioning panel inserted to the right) or red/blue (*Z* plane sectioning inserted in the top) lines. The fluorescence imaging was overlaid on top of the differential interference contrast image (DIC) in order to have a relative view of the cell together with the labeled vesicles.

stability profile without further additives or special storage conditions.

DISCUSSION

Several vectors have been utilized to enhance the delivery of ONs. Cationic liposomes have been extensively studied for this purpose; however, despite demonstrating high activity, the associated toxicity has hindered their progress into clinical applications (13). Alternatively, CPPs have been shown to deliver a wide variety of nucleic acid-based therapeutics intracellularly, including SCOs and siRNA (14,29). CPPs covalently conjugated to SCOs have been shown to induce splice-correction activity in different models (7,16). However, this strategy entails laborious chemical conjugation procedures (19). In addition, high doses of the SCO are required to induce significant biological response (17). On the other hand, some CPPs have shown to be able to deliver ONs utilizing a non-covalent complexation strategy, especially when chemically modified with fatty acids (18,20). We have demonstrated earlier that the stearylated versions of TP10 (21) and (RXR)4 (17) show enhanced ability to deliver SCOs and plasmids into cells upon non-covalent

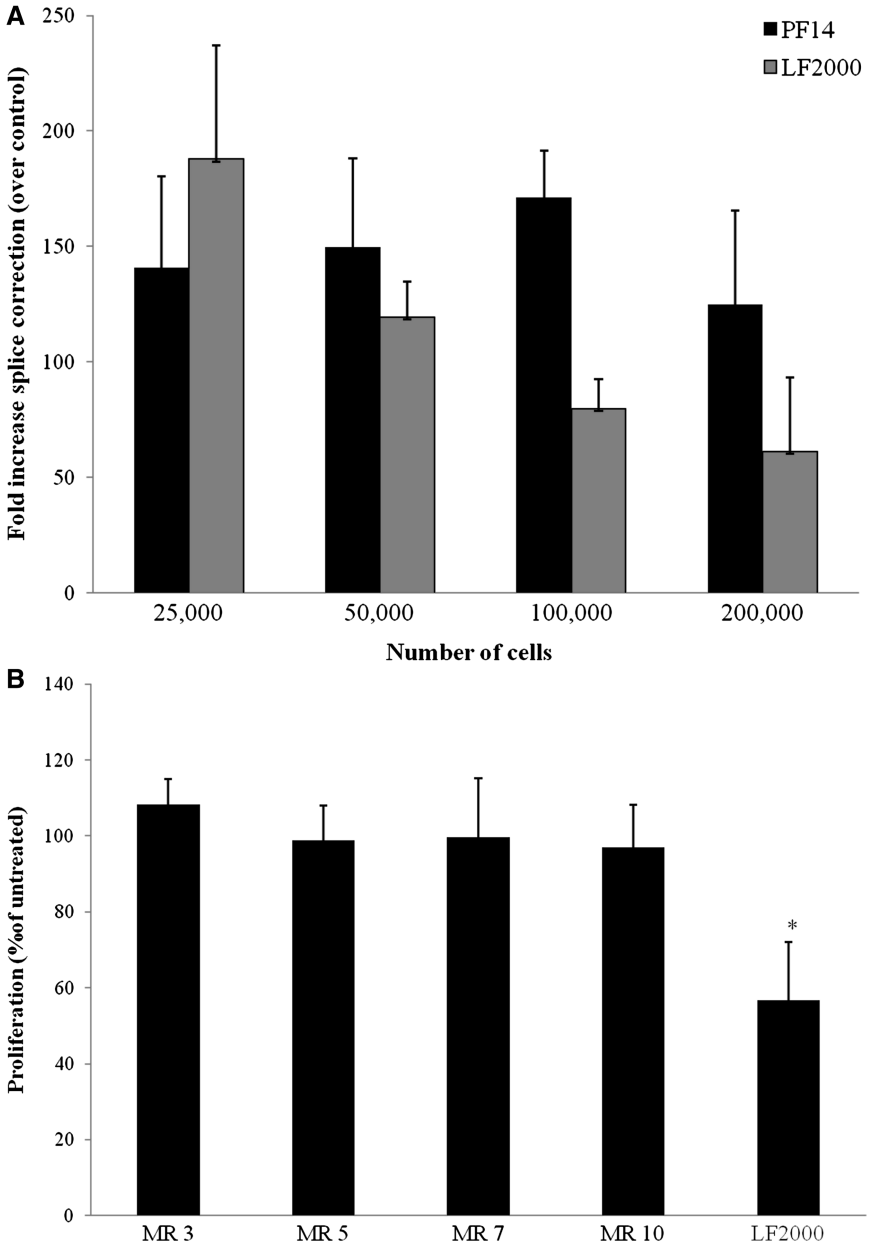

Figure 5. Cell confluency dependence and cytotoxicity. (**A**) HeLa pLuc705 cells seeded at indicated densities 1 day prior to the experiment were treated with 200 nM SCO with either PF14 MR5 or LF2000. (**B**) Cells were exposed to PF14 (MR5, SCO 200 nM) complexes for 4 h in serum-free medium, followed by addition of serum to a final concentration of 10% and incubated for additional 20 h. LF2000 was used according to the manufacturer's protocol in serum-free conditions with the same SCO dose. Splice-correction assay results are presented as fold-increase untreated cells (control). Toxicity was assessed by Wst-1 assay. The values represent the mean of at least three independent experiments performed in duplicate (mean ± SEM, $n = 3$). Intergroup differences were considered significant at $^*P < 0.05$ using Student's *t*-test.

complexation. In contrast to other CPPs that are predominantly entrapped in endosomal vesicles after internalization, the remarkably enhanced splice-correction observed with stearyl-TP10 and stearyl-(RXR)4 was mainly due to more efficient endosomal escape (17,21). However, despite being less toxic than lipid-based vectors such as LF2000, these peptides are generally less efficient. Moreover, most transfection reagents are highly active in serum-free conditions, but show considerable decrease in their efficiency in the presence of serum. This is important, since it immediately suggests that they are less likely to perform well *in vivo*.

In the current work we present a new chemically modified CPP, PF14. Starting from stearyl-TP10, we utilized ornithines as the main source of positive charges instead of lysines. The design of this peptide was based on earlier reports showing that poly-L-ornithine demonstrated superior transfection efficiency (up to 10-fold) compared to equivalent poly-L-lysine-based systems (30). The superior efficiency of poly-L-ornithines was related to

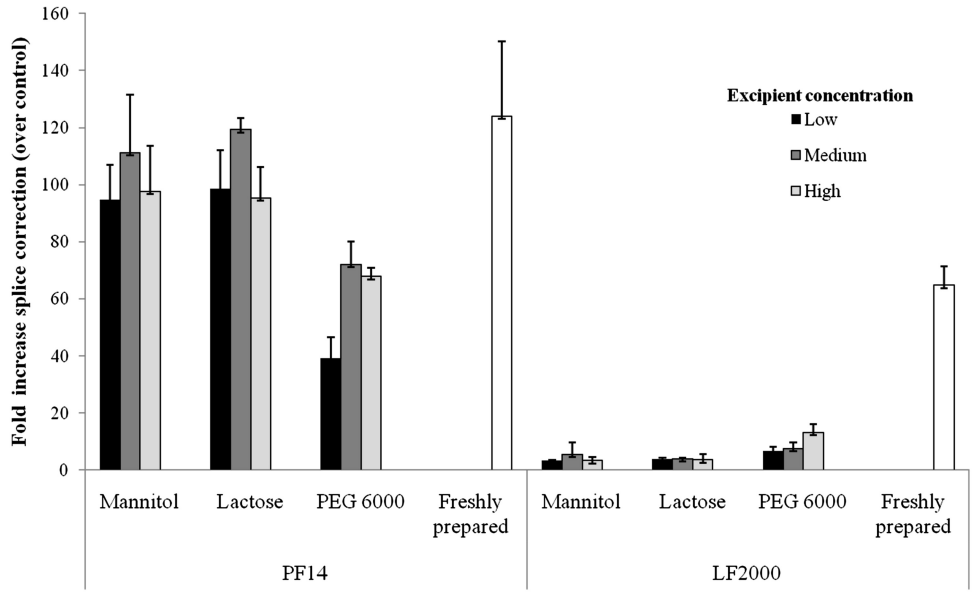

Figure 6. Solid formulation development and excipient screening. Excipient solutions of lactose, mannitol and PEG 6000 were prepared at final concentration of 100 mg/ml in MQ water. PF14-SCO nanocomplexes were prepared in 25 µl MQ water for 1 h, then different proportions of the excipient solutions were added to the final concentrations of 1.67% (low), 3.33% (medium) and 5% (high) solubilized excipient in the reaction mixture. The mixture was then dried in speed-vac for 2 h, during which the temperature ranged between 55 and 60°C. Before transfection, the dried powder was reconstituted in 50 µl of MQ water and added to the wells. LF2000 complexes were prepared according to manufacturer's protocol. Subsequently, the same proportions of the excipient solutions utilized for PF14 formulation were added, and the mixture was dried and reconstituted similarly. HeLa pLuc705 cells (5×10^4) were treated with reconstituted complexes for 24 h in serum containing medium. Cells were then lysed in 0.1% Triton X-100 and luciferase activity was measured. The results from splice-correction assay of different formulations of PF14 and LF2000 are presented as fold-increase over untreated cells (control).

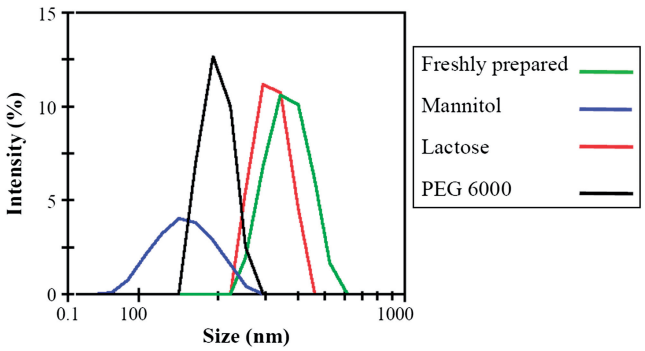

Figure 7. Dynamic light scattering (DLS). Average diameter of the particles formed by the different formulations studied. Particle size distribution was assessed by dynamic light scatter. All samples were measured in triplicates. The figure shows representative curves of the populations' distribution in relation to intensity of the scattered light. All formulations were used at the concentration of 3.33%.

Table 2. Average diameter of the population of complexes in 0.01 mM KCl or in the presence of 10% serum

Samples	Average diameter (nm)	Zeta potential (mV) in 0.01mM KCl	Zeta potential (mV) in OptiMEM 10% FCS
Freshly prepared	363.8 ± 52	−28.4 ± 3.79	−12.1 ± 1.41
Mannitol	156.9 ± 43.7	−15.4 ± 6.31	−14.2 ± 1.64
Lactose	298 ± 57.7	−16.4 ± 4.37	−10.4 ± 2.06
PEG 6000	208.3 ± 76	−17.7 ± 1.72	−9.94 ± 2.55

Average peak is presented in nm (STD). All solid dispersion formulations were used at the concentration 3.33%.

the higher affinity for DNA and the ability to make more stable complexes at lower charge ratios (30). Furthermore, we hypothesized that ornithine, being a nonstandard amino acid, would be less prone to serum proteases, and thus could retain the activity in serum conditions.

Upon screening for the most optimal MR in the HeLa pLuc705 cell model, we found that MR5 displayed the highest activity in serum-free and serum-containing media (Figure 1). Importantly, in contrast to all tested CPPs so far, PF14 displayed higher activity than LF2000 even in the presence of serum. PF14 activity also exceeded that of Oligofectamine™, RNAiMAX™ and jetPEI™ (Supplementary Figure S2). When used at the same concentration, stearyl-TP10 imparted modest activity compared to PF14, which demonstrates the importance of the new modifications (Figure 1). Also, removal of the stearyl group abolished the activity entirely (Figure 1), emphasizing the role of such a lipophilic moiety. On the mRNA level, PF14-SCO nanocomplexes had a very low EC_{50} value of ~100 nM in both types of media (Figure 2A). Compared to other reported CPPs such as Pip1, RXR4 and R6Pen covalently linked to splice correcting PNA (7), PF14-SCO nanocomplexes had at least five times lower EC_{50} values. These results add to the evidence that non-covalent complexation imparts biological activity at lower ON concentrations. Kinetics studies showed early onset of activity.

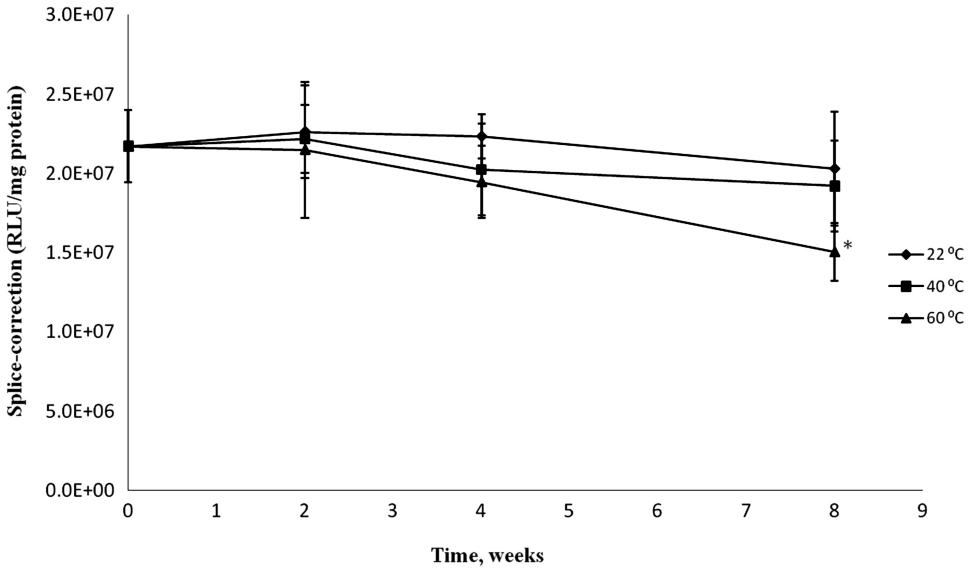

Figure 8. Stability testing. Lactose-SD 3.33% formulations were stored either at RT (22°C) or in ovens of adjusted temperatures (40 and 60°C). Samples were monitored for 8 weeks and tested at 0, 2, 4 and 8 weeks. Measurements were carried out in triplicates and differences were considered significant at $*P < 0.05$ according to Student's *t*-test.

More than 60% splice-correction was achieved as early as 8 h after transfection. This demonstrates that, despite being very stable, the nanocomplexes are rapidly dissociated inside the cells releasing SCO cargo. However, natural decline in the signal takes place after 48 h as the nanocomplexes become more dilute due to degradation and cell division (31). In line with the above-mentioned reports (30), our results suggest that ornithine forms very stable nanocomplexes that are more resistant to cellular and serum proteases enabling PF14 to mediate very high levels of splice-correction much more efficiently than its predecessor; stearyl TP-10.

To demonstrate the activity of PF14 in a disease-relevant model, we used mdx mouse myotubes, a model for DMD. Remarkably, PF14 nanocomplexes were able to induce significant levels of splice-correction exceeding LF2000 at MR7 (Figure 3C). Compared to other peptide-based vectors tested in the same model, PF14 is significantly more active reaching saturation of the corrected band signal at doses ranging from 250 nM for MR5 and 200 nM for MR7, which is several folds lower than doses in the micromolar range used for other vectors (7). Additionally, PF14 effect was not substantially affected in the presence of serum.

To quantify the efficiency of uptake of SCOs by PF14, fluorescently labeled (Cy5) SCO was used in complex formation. The quantitative uptake assay helps to clarify the relation between the amount of the internalized complexes and their biological activity. Interestingly, despite the congruency between the uptake data and the splice-correction data in the absence of chloroquine, splice-correction was significantly increased in the presence of chloroquine (Figure 4A). We have reported on similar patterns for stearyl-TP10 (21). These data show that, although PF14 nanocomplexes display very efficient splice-correction activity, some of the complexes are entrapped in endosomes and are released after endosomal rupture in the presence of chloroquine. However, despite the increased efficiency of PF14 in the presence of chloroquine, its basal activity levels are much higher than those of stearyl-TP10 and LF2000. This proves that PF14 is a very efficient delivery vector; however, there is space for improvement of its activity by further enhancement of endosomal escape. To corroborate the role of endocytosis in the uptake of PF14 nanocomplexes, transfections were carried out at lowered temperature (4°C), which is supposed to halt energy-dependent processes like endocytosis. As expected, the transfection efficiency of PF14 was markedly decreased at 4°C, indicating the involvement of endocytic processes in the uptake (Figure 4B). To visualize this process fluoresceinyl-labeled dextran, a marker for endocytosis (32), was used. Co-localization between labeled dextran and Cy5-labeled SCO in the cytoplasm strongly suggests a prominent role of endocytosis in the uptake of PF14 nanocomplexes (Figure 4C and Supplementary Figure S3).

Further characterization of the efficiency of PF14 was done utilizing flow-cytometry to assess the percentage of cells being transfected. Importantly, PF14 was able to transfect nearly 100% of the cell population (Supplementary Figure S4), which explains the nearly 90% correction observed after 24 h with RT–PCR (Figure 2B). Upon testing PF14 over an increasing cell density, it showed less sensitivity than LF2000 towards variations in cell confluency (Figure 5A). This is very important for *in vitro* screens that require different endpoints and for successful *in vivo* implementation where the target is intact tissues. Comparing the cytotoxicity of both vectors through the activity of mitochondrial dehydrogenases showed that PF14 had no impact on the cell viability and was significantly less toxic than LF2000 even in serum-free conditions (Figure 5B).

Finally, we wanted to take our delivery system a step further by developing a suitable formulation for administration. The formulation process is an indispensable step for the development of any therapeutic product. It has great effect on enhancing the efficiency and stability of active pharmaceutical ingredients. Additionally, specific formulations have to be tailored for different therapeutic approaches. Among the different pharmaceutical forms present, solid formulations remain the most widely used. It is the form used in tablets, capsules, powders for inhalation and even powders for injection. This is because they are easy to handle and very stable upon storage and transportation. Although CPPs have been extensively exploited in recent years for the delivery of various therapeutics (15), to our knowledge, formulation of CPPs into different pharmaceutical forms has never been thoroughly studied. Therefore, to expand the range of therapeutic applications of CPP-based therapeutics, there is a need for studies exploring the possibility of incorporating CPPs in different pharmaceutical forms; especially the solid form. To test the feasibility of formulating PF14-SCO complexes into solid formulation, solid dispersion technique was utilized. Although initially invented to increase the solubility of poorly water-soluble drugs by dispersing them over hydrophilic solid matrices (33), it is not used for the same purpose in the present work. This is because PF14-SCO complexes are already water-soluble. However, the technique was adopted to enable us obtain uniform distribution of the nanocomplexes over water-soluble excipients by solvent evaporation. For solvent evaporation (in this case water), we chose speed drying under elevated temperature (55–60°C) and reduced pressure. Despite being relatively stressful drying method, it is more relevant to the widely used, cost-effective, heat-based pharmaceutical drying techniques. As shown in Figure 6, we found that that lactose-SD 3.33% was the most optimal formulation, achieving splice-correction activity similar to that of the freshly prepared complexes in solution. Mannitol solid dispersions mediated lower activity, while PEG formulations were the least active. It was clear that different excipients and concentrations thereof had a huge impact on the activity of the formulation. This suggests that excipients affect the nanocomplexes in different ways. The nanocomplexes are formed by non-covalent electrostatic interactions with the ON. Therefore, different excipients varying in their surface charge distribution could interfere with these interactions affecting the physicochemical properties of the nanocomplexes and eventually the biological activity. However, an excipient concentration of 3.33% is shown to be relatively superior in all the excipients tested, which suggests that there is an optimal ratio between the concentration of nanocomplexes in solution and the amount of solubilized solid material. On the contrary, LF2000 almost lost its entire activity upon application of this drying and dispersion procedure (Figure 6). The success of PF14-SCO complexes to withstand harsh drying and dispersion procedure at which the widely used commercial lipid-based vector failed suggests that PF14-SCO nanocomplexes are physicochemically more stable than the lipoplexes, yet biologically more active. Additionally, we characterized the effect of formulation on the kinetics of splice correction obtained by the best formulation (lactose-SD 3.33%). We found that it demonstrated similar kinetic profile to the freshly prepared nanocomplexes (Supplementary Figure S5).

In order to assess that the presence of intact nanocomplexes after the formulation procedure, DLS studies were performed comparing the freshly prepared nanocomplexes with the solid formulations obtained after drying at 50–60°C . We found that the particles size and particle-size distribution is highly affected by the type of excipient used (Figure 7 and Table 2). Lactose-SD 3.33% formulation, which mediated the highest splice-correction activity, also had DLS profile most similar to the freshly prepared nanocomplexes. This proves that the choice of excipient for formulation of such nanocomplexes is an extremely important step that affects both their physicochemical properties and biological activity. Yet, another physicochemical property that could affect the biological activity is the zeta potential. Particles of different surface charge are expected to have distinct interactions with the plasma membrane, which should affect the uptake mechanism and efficiency of the delivery vector. We expected that a cationic CPP-based nanocomplex should possess net positive surface charge. Surprisingly however, we found that all the nanocomplexes, either freshly prepared or in solid formulation, with or without serum, possessed a net negative charge. The efficiency of such nanocomplexes can be explained in light of earlier research on lipoplexes showing that cationic liposome and plasmid DNA complexes are negatively charged under optimal transfection conditions (34) and that this holds *in vivo* as well (35). In further research studying the uptake mechanisms of CPPs it will be interesting to elucidate how this net negative charge affects the interaction with the plasma membrane and the biological activity.

Next, we subjected the best performing formulation, lactose-SD 3.33%, to stressful stability testing conditions at elevated temperatures for 2 months. Storage at high temperatures increases the rate of degradation reactions that could take years to occur (36). For this reason this method is routinely used to assess the long-term stability of formulations (27,28,37–39). Lactose-SD 3.33% formulation demonstrated high stability over the tested time period with no significant loss in transfection efficiency at most of the time points (Figure 8). The only significant decrease in activity was the 60°C 8-weeks time point, where it was ~70% of the initial activity. However, this is a remarkably good stability profile for a plain formulation without any type of preservatives, coating or special packaging. In addition, these results further corroborate the high stability of PF14 nanocomplexes. In comparison with solid formulation of lipoplexes, PF14 nanocomplexes demonstrate very good activity and stability profiles. Earlier reports showing that lipoplexes could be dried over solid matrices mainly utilized the freeze-drying technique in the presence of lyoprotectant sugars like trehalose, mannitol or sucrose (38–40). However, despite using sufficient levels of lyoprotectant sugars, significant damage was still evident when dilute lipoplex preparations were subjected to freeze-drying (28). This damage occurs

during the freezing step, and sugars have a limited capacity to protect against freezing-induced damage (28). Furthermore, industrially, the freeze-drying (lyophilization) process is known to be much more cumbersome and costly than the conventional heat-based pharmaceutical drying procedure. Additionally, it was shown that the lyophilized lipoplexes suffered progressive loss in transfecetion efficiency when subjected to stability settings similar to what we have used in the present study (27). The degradation was mainly due to the generation of reactive-oxygen species and was increased in the presence of metal contaminants (27,37). Consequently, chelators were used to enhance the stability profile; however, the effects of these additives on vector stability during lyophilization are difficult to predict (37). To our knowledge, PF14 is the first vector reported to retain nearly 100% of its transfection efficiency utilizing a heat-based drying and dispersion procedure. Furthermore, PF14 showed a very good stability profile in the absence of additional formulation requirements.

In conclusion, we have shown that the chemically modified CPP, PF14, is able to efficiently deliver SCOs to different cell-lines including a disease-relevant hard-to-transfect cell-line, H2K. Furthermore, we have successfully been able to formulate PF14-SCO nanocomplexes into solid formulation utilizing the solid dispersion technique using a convenient heat-based drying method. The solid formulations demonstrated splice-correction activity almost identical to the freshly prepared nanocomplexes; however, this efficiency was sensitive to the type of excipient used and its concentration. The nanocomplexes remained intact after formulation and the formulation remained active even when subjected to stressful stability conditions for 2 months. Importantly, being able to formulate PF14 nanocomplexes into an active and stable solid formulation is an important proof-of-principle that CPP-based therapeutics could be incorporated in solid pharmaceutical forms. This could significantly extend the horizon of therapeutic applications of CPPs. Collectively, our results suggest that PF14 is a promising translational approach for delivering SCOs in different pharmaceutical forms and opens new opportunities to develop more pharmaceutically relevant assays for CPPs.

SUPPLEMENTARY DATA

Supplementary Data are available at NAR Online.

ACKNOWLEDGEMENTS

We would like to thank Johanna Unger for her assistance in the preparation of the initial experiments. The confocal imaging study was performed at the Live Cell Imaging unit, Department of Biosciences and Nutrition, Karolinska Institutet, Huddinge, Sweden.

FUNDING

Swedish Research Council (VR-NT); VINNOVA-SAMBIO joint project; SSF (Sweden-Japan); Center for Biomembrane Research, Stockholm; Knut and Alice Wallenberg's Foundation; the EU trough the European Regional Development Fund through the Center of Excellence in Chemical Biology, Estonia; the targeted financing SF0180027s08 from the Estonian Government; the DoRa Program of The European Social Fund; Archimedes Foundation; the Torsten and Ragnar Söderberg Foundation; KI faculty funds for funding of postgraduated students (to J.R.V.); Egyptian Ministry of Higher Education (to E.M.Z.); Swedish Society of Medical Research (SSMF to S.E.A.); Work in the Gait laboratory is supported by the Medical Research Council (Unit program U105178803). Funding for open access charge: Swedish Research Council (VR-NT).

Conflict of interest statement. None declared.

REFERENCES

1. Munos,B. (2009) Lessons from 60 years of pharmaceutical innovation. *Nat. Rev. Drug Discov.*, **8**, 959–968.
2. Butler,D. (2008) Translational research: crossing the valley of death. *Nature*, **453**, 840–842.
3. Nilsen,T.W. and Graveley,B.R. (2010) Expansion of the eukaryotic proteome by alternative splicing. *Nature*, **463**, 457–463.
4. Sazani,P. and Kole,R. (2003) Therapeutic potential of antisense oligonucleotides as modulators of alternative splicing. *J. Clin. Invest.*, **112**, 481–486.
5. Bauman,J., Jearawiriyapaisarn,N. and Kole,R. (2009) Therapeutic potential of splice-switching oligonucleotides. *Oligonucleotides*, **19**, 1–13.
6. Wood,M.J. (2010) Toward an oligonucleotide therapy for duchenne muscular dystrophy: a complex development challenge *Sci. Transl. Med.*, **2**, 25ps15.
7. Ivanova,G.D., Arzumanov,A., Abes,R., Yin,H., Wood,M.J., Lebleu,B. and Gait,M.J. (2008) Improved cell-penetrating peptide-PNA conjugates for splicing redirection in HeLa cells and exon skipping in mdx mouse muscle. *Nucleic Acids Res.*, **36**, 6418–6428.
8. van Deutekom,J.C., Janson,A.A., Ginjaar,I.B., Frankhuizen,W.S., Aartsma-Rus,A., Bremmer-Bout,M., den Dunnen,J.T., Koop,K., van der Kooi,A.J., Goemans,N.M. *et al.* (2007) Local dystrophin restoration with antisense oligonucleotide PRO051. *N. Engl. J. Med.*, **357**, 2677–2686.
9. Kinali,M., Arechavala-Gomeza,V., Feng,L., Cirak,S., Hunt,D., Adkin,C., Guglieri,M., Ashton,E., Abbs,S., Nihoyannopoulos,P. *et al.* (2009) Local restoration of dystrophin expression with the morpholino oligomer AVI-4658 in duchenne muscular dystrophy: a single-blind, placebo-controlled, dose-escalation, proof-of-concept study. *Lancet Neurol.*, **8**, 918–928.
10. Bell,N.M. and Micklefield,J. (2009) Chemical modification of oligonucleotides for therapeutic, bioanalytical and other applications. *Chembiochem*, **10**, 2691–2703.
11. Amidon,G.L., Lennernas,H., Shah,V.P. and Crison,J.R. (1995) A theoretical basis for a biopharmaceutic drug classification: the correlation of in vitro drug product dissolution and in vivo bioavailability. *Pharm. Res.*, **12**, 413–420.
12. Lipinski,C.A., Lombardo,F., Dominy,B.W. and Feeney,P.J. (2001) Experimental and computational approaches to estimate solubility and permeability in drug discovery and development settings. *Adv. Drug Deliv. Rev.*, **46**, 3–26.
13. Dass,C.R. (2004) Lipoplex-mediated delivery of nucleic acids: factors affecting in vivo transfection. *J. Mol. Med.*, **82**, 579–591.
14. Ezzat,K., El Andaloussi,S., Abdo,R. and Langel,Ü. (2010) Peptide-based matrices as drug delivery vehicles. *Curr. Pharm. Des.*, **16**, 1167–1178.
15. Heitz,F., Morris,M.C. and Divita,G. (2009) Twenty years of cell-penetrating peptides: from molecular mechanisms to therapeutics. *Br. J. Pharmacol.*, **157**, 195–206.

16. Wood,M.J., Gait,M.J. and Yin,H. (2010) RNA-targeted splice-correction therapy for neuromuscular disease. *Brain*, **133**, 957–972.
17. Lehto,T., Abes,R., Oskolkov,N., Suhorutsenko,J., Copolovici,D.M., Mäger,I., Viola,J.R., Simonson,O.E., Ezzat,K., Guterstam,P. *et al.* (2010) Delivery of nucleic acids with a stearylated (RxR)4 peptide using a non-covalent co-incubation strategy. *J. Control. Release*, **141**, 42–51.
18. Deshayes,S., Morris,M., Heitz,F. and Divita,G. (2008) Delivery of proteins and nucleic acids using a non-covalent peptide-based strategy. *Adv. Drug Deliv. Rev.*, **60**, 537–547.
19. Mäe,M., Andaloussi,S.E., Lehto,T. and Langel,Ü. (2009) Chemically modified cell-penetrating peptides for the delivery of nucleic acids. *Expert Opin. Drug Deliv.*, **6**, 1195–1205.
20. Futaki,S., Ohashi,W., Suzuki,T., Niwa,M., Tanaka,S., Ueda,K., Harashima,H. and Sugiura,Y. (2001) Stearylated arginine-rich peptides: a new class of transfection systems. *Bioconjug. Chem.*, **12**, 1005–1011.
21. Mäe,M., El Andaloussi,S., Lundin,P., Oskolkov,N., Johansson,H.J., Guterstam,P. and Langel,Ü. (2009) A stearylated CPP for delivery of splice correcting oligonucleotides using a non-covalent co-incubation strategy. *J. Control. Release*, **134**, 221–227.
22. Guterstam,P., Lindgren,M., Johansson,H., Tedebark,U., Wengel,J., El Andaloussi,S. and Langel,Ü. (2008) Splice-switching efficiency and specificity for oligonucleotides with locked nucleic acid monomers. *Biochem. J.*, **412**, 307–313.
23. Lu,Q.L., Rabinowitz,A., Chen,Y.C., Yokota,T., Yin,H., Alter,J., Jadoon,A., Bou-Gharios,G. and Partridge,T. (2005) Systemic delivery of antisense oligoribonucleotide restores dystrophin expression in body-wide skeletal muscles. *Proc. Natl Acad. Sci. USA*, **102**, 198–203.
24. Coin,I., Beyermann,M. and Bienert,M. (2007) Solid-phase peptide synthesis: from standard procedures to the synthesis of difficult sequences. *Nat. Protoc.*, **2**, 3247–3256.
25. Morgan,J.E., Beauchamp,J.R., Pagel,C.N., Peckham,M., Ataliotis,P., Jat,P.S., Noble,M.D., Farmer,K. and Partridge,T.A. (1994) Myogenic cell lines derived from transgenic mice carrying a thermolabile T antigen: a model system for the derivation of tissue-specific and mutation-specific cell lines. *Dev. Biol.*, **162**, 486–498.
26. Kang,S.H., Cho,M.J. and Kole,R. (1998) Up-regulation of luciferase gene expression with antisense oligonucleotides: implications and applications in functional assay development. *Biochemistry*, **37**, 6235–6239.
27. Molina,M.D. and Anchordoquy,T.J. (2008) Degradation of lyophilized lipid/DNA complexes during storage: the role of lipid and reactive oxygen species. *Biochim. Biophys. Acta*, **1778**, 2119–2126.
28. Yu,J. and Anchordoquy,T.J. (2009) Synergistic effects of surfactants and sugars on lipoplex stability during freeze-drying and rehydration. *J. Pharm. Sci.*, **98**, 3319–3328.
29. El Andaloussi,S., Lehto,T., Mäger,I., Rosenthal-Aizman,K., Oprea,J., Simonson,O.E., Sork,H., Ezzat,K., Copolovici,D.M., Kurrikoff,K. *et al.* (2011) Design of a peptide-based vector, PepFect6, for efficient delivery of siRNA in cell culture and systemically in vivo. *Nucleic Acids Res.*, doi:10.1093/nar/gkq1299 [Epub ahead of print].
30. Ramsay,E. and Gumbleton,M. (2002) Polylysine and polyornithine gene transfer complexes: a study of complex stability and cellular uptake as a basis for their differential in-vitro transfection efficiency. *J. Drug Target.*, **10**, 1–9.
31. Hällbrink,M., Oehlke,J., Papsdorf,G. and Bienert,M. (2004) Uptake of cell-penetrating peptides is dependent on peptide-to-cell ratio rather than on peptide concentration. *Biochim. Biophys. Acta*, **1667**, 222–228.
32. Alam,M.R., Dixit,V., Kang,H., Li,Z.B., Chen,X., Trejo,J., Fisher,M. and Juliano,R.L. (2008) Intracellular delivery of an anionic antisense oligonucleotide via receptor-mediated endocytosis. *Nucleic Acids Res.*, **36**, 2764–2776.
33. Vasconcelos,T., Sarmento,B. and Costa,P. (2007) Solid dispersions as strategy to improve oral bioavailability of poor water soluble drugs. *Drug Discov. Today*, **12**, 1068–1075.
34. Son,K.K., Patel,D.H., Tkach,D. and Park,A. (2000) Cationic liposome and plasmid DNA complexes formed in serum-free medium under optimum transfection condition are negatively charged. *Biochim. Biophys. Acta*, **1466**, 11–15.
35. Son,K.K., Tkach,D. and Hall,K.J. (2000) Efficient in vivo gene delivery by the negatively charged complexes of cationic liposomes and plasmid DNA. *Biochim. Biophys. Acta*, **1468**, 6–10.
36. Ahuja,S. and Scypinski,S. (2001) *Handbook of Modern Pharmaceutical Analysis*. Academic Press, San Diego.
37. Molina,M.C. and Anchordoquy,T.J. (2007) Metal contaminants promote degradation of lipid/DNA complexes during lyophilization. *Biochim. Biophys. Acta*, **1768**, 669–677.
38. Armstrong,T.K. and Anchordoquy,T.J. (2004) Immobilization of nonviral vectors during the freezing step of lyophilization. *J. Pharm. Sci.*, **93**, 2698–2709.
39. Molina,M.C., Armstrong,T.K., Zhang,Y., Patel,M.M., Lentz,Y.K. and Anchordoquy,T.J. (2004) The stability of lyophilized lipid/DNA complexes during prolonged storage. *J. Pharm. Sci.*, **93**, 2259–2273.
40. Brus,C., Kleemann,E., Aigner,A., Czubayko,F. and Kissel,T. (2004) Stabilization of oligonucleotide-polyethylenimine complexes by freeze-drying: physicochemical and biological characterization. *J. Control. Release*, **95**, 119–131.